



# Synthesis, biological activity, and biopharmaceutical characterization of tacrine dimers as acetylcholinesterase inhibitors



Shuai Qian<sup>a,b</sup>, Lisi He<sup>c</sup>, Marvin Mak<sup>d</sup>, Yifan Han<sup>d</sup>, Chun-Yu Ho<sup>c,e,\*\*</sup>, Zhong Zuo<sup>a,\*</sup>

<sup>a</sup> School of Pharmacy, Faculty of Medicine, The Chinese University of Hong Kong, Shatin, New Territories, Hong Kong Special Administrative Region

<sup>b</sup> School of Traditional Chinese Medicine, China Pharmaceutical University, Nanjing, PR China

<sup>c</sup> Department of Chemistry, The Chinese University of Hong Kong, Shatin, New Territories, Hong Kong Special Administrative Region

<sup>d</sup> Department of Applied Biology and Chemical Technology, Institute of Modern Chinese Medicine, The Hong Kong Polytechnic University, Hung Hom, Hong Kong Special Administrative Region

<sup>e</sup> Department of Chemistry, South University of Science and Technology of China, Shenzhen, PR China

## ARTICLE INFO

### Article history:

Received 20 May 2014

Received in revised form 19 September 2014

Accepted 26 October 2014

Available online 31 October 2014

### Keywords:

Tacrine

Dimers

Acetylcholinesterase

Cytotoxicity

Permeability

## ABSTRACT

Tacrine (THA), as the first approved acetylcholinesterase (AChE) inhibitors for the treatment of Alzheimer's disease (AD), has been extensively investigated in last seven decades. After dimerization of THA via a 7-carbon alkyl spacer, bis(7)-tacrine (B7T) showed much potent anti-AChE activity than THA. We here report synthesis, biological evaluation and biopharmaceutical characterization of six THA dimers referable to B7T. According to IC<sub>50</sub> values, the *in vitro* anti-AChE activities of THA dimers were up to 300-fold more potent and 200-fold more selective than that of THA. In addition, the anti-AChE activities of THA dimers were found to be associated with the type and length of the linkage. All studied THA dimers showed much lower cytotoxicity than B7T, but like B7T, they demonstrated much lower absorptive permeabilities than that of THA on Caco-2 monolayer model. In addition, all THA dimers demonstrated significant efflux transport (efflux ratio >4), indicating that the limited permeability could be associated with the efflux transport during absorption process. Moreover, the dimer with higher Log *P* value was accompanied with higher permeability but lower aqueous solubility. A balanced consideration of activity, solubility, cytotoxicity and permeability should be conducted in selection of the potential candidates for further *in vivo* investigation.

© 2014 Elsevier B.V. All rights reserved.

## 1. Introduction

Alzheimer's disease (AD), as the most common form of dementia, is a chronic and neurodegenerative disease that attacks the brain and leads to the impaired memory, thinking and behavior in the elderly. AD has been proven to be a multifactorial disease associated with several aspects including cholinergic deficiency, glutamate induced excitotoxicity, formation of  $\beta$ -amyloid (A $\beta$ ) precipitates, oxidative stress, tau hyperphosphorylation and so on (Goedert and Spillantini, 2006; Heppner et al., 2004). The neuropathological alterations described above suggest the possible treatment of AD could come from drugs that can target at these

factors. For the past decade the cholinergic approach has been the first and the most frequently used therapeutic strategy for the treatment of mild to moderate AD. Levels of acetylcholine can be enhanced by inhibiting acetylcholinesterase (AChE) with reversible inhibitors. The AChE inhibitors (AChEIs) were found to be the only ones that could produce significant and reproducible therapeutic effects (Standridge, 2004). Since mid-1990s, only four AChEIs, namely tacrine (THA), donepezil, rivastigmine and galantamine, have been approved by the FDA in US for the treatment of AD (Standridge, 2004). Huperzine, a novel *Lycopodium* alkaloid chemically unique from other known AChEIs for AD, was first discovered in a Chinese medicinal herb *Huperzia serrate*. The agent has been approved for AD in China because of its potent memory-enhancing effects, specific anti-AChE activity, and fewer side effects (Tang and Han, 1999). In addition to targeting cholinergic deficiency, reducing glutamate induced excitotoxicity by *N*-methyl-D-aspartate receptor antagonists (e.g., FDA approved memantine) (Reisberg et al., 2003), and preventing the build-up of A $\beta$  by  $\beta$ -secretase 1 (BACE 1) inhibitors (e.g., MK-8931, LY2886721 in clinical trials) also severed two kinds of treatments

\* Corresponding author at: School of Pharmacy, Faculty of Medicine, The Chinese University of Hong Kong, Shatin, New Territories, Hong Kong Special Administrative Region. Tel.: +852 3943 6832; fax: +852 2603 5295.

\*\* Corresponding author at: Department of Chemistry, South University of Science and Technology of China, Shenzhen, PR China. Tel.: +86 755 8801 8318.

E-mail addresses: [jasonhcy@sustc.edu.cn](mailto:jasonhcy@sustc.edu.cn) (C.-Y. Ho), [joanzuo@cuhk.edu.hk](mailto:joanzuo@cuhk.edu.hk) (Z. Zuo).

of AD. However, none of above strategies could completely prevent the neurodegeneration and cure the AD till now (Evin et al., 2011; Robinson and Keating, 2006; Terry and Buccafusco, 2003), which may be due to that they only focused on one targeting site of drug action. As a consequence, drug discovery in AD is gradually moving from the development of molecules with a single target to the “multi-target-directed ligands” (MTDLs), which is capable to simultaneously address several key pathophysiological processes as described above (Bajda et al., 2011; Cavalli et al., 2008). Recently, Voisin et al. reported a well-controlled clinical trial of memantine (NMDA receptor antagonist)/donepezil (AChEI) dual therapy. They found that combination of donepezil and memantine has superior efficacy than donepezil alone in the severe AD subgroup, potentially supporting a role for dual treatment in more advanced AD patients (Voisin et al., 2004). Such clinical findings also support the multi-target strategy for the treatment of AD.

Accordingly, commercial AChEIs have been widely investigated and modified with additional features, in order to solve the issue of both cholinergic deficiency and other above-mentioned targets in AD. As the first approved AChEI drug, THA was the most extensively investigated drug. Many efforts have been concentrated on the synthesis of its derivatives as MTDLs for AD treatment (Bajda et al., 2011) due to its high anti-AChE activity, much low molecular weight (MW: 198, lower than other approved AChEIs) and potential attenuating A $\beta$ -induced neurotoxicity (Svensson and Nordberg, 1998). Over the past decade, various THA derivatives have been developed and indeed demonstrated multi-target properties *in vitro* and in animal models, including inhibition of

AChE, BACE1, A $\beta$  aggregation and reactive oxygen species as well as blockade of NMDA receptor and nitric oxide synthase, etc. (Alcala Mdel et al., 2003; Alonso et al., 2005; Chao et al., 2012; Fu et al., 2007, 2008; Li et al., 2006; Minarini et al., 2012; Pi et al., 2012).

Bis(7)-tacrine (B7T), a dimeric THA analog designed with the aid of computer docking program and synthesized by our research group (Fig. 1b), is a promising anti-AD candidate with multi-potencies including anti-NMDA receptors, anti-nitric oxide synthase signaling, and the reduction of A $\beta$  neurotoxicity in addition to high potency and selectivity on AChE inhibition (Fu et al., 2007; Li et al., 2005, 2006, 2007, 2009). Following a single oral administration to rats, B7T showed significantly improved *in vivo* brain AChE inhibition, reduced *in vivo* serum BChE inhibition, and fewer peripheral cholinergic side effects than that of THA (Wang et al., 1999b). In addition, B7T could ameliorate learning and memory impairment induced by scopolamine (Wang et al., 1999a), AF64A (Liu et al., 2000), or permanent ligation of the bilateral common carotid arteries (Shu et al., 2012) in the Morris Water maze. However, the oral bioavailability of B7T was very low (~10%) in rats mainly due to its high lipophilicity (Log *P*=8.2 (Yu et al., 2008)), poor intestinal permeability and significant tissue binding (Zhang et al., 2008). Similar to B7T, HLS-1 and HLS-2 (Fig. 1), designed by Bolognesi et al., also demonstrated multi-target properties via inhibiting AChE, reversing AChE-induced amyloid fibrillogenesis and acting as metal chelators (Bolognesi et al., 2007).

Currently, hundreds of novel AChEIs have been synthesized and investigated (Bajda et al., 2011; Mehta et al., 2012; Tumiatti et al.,

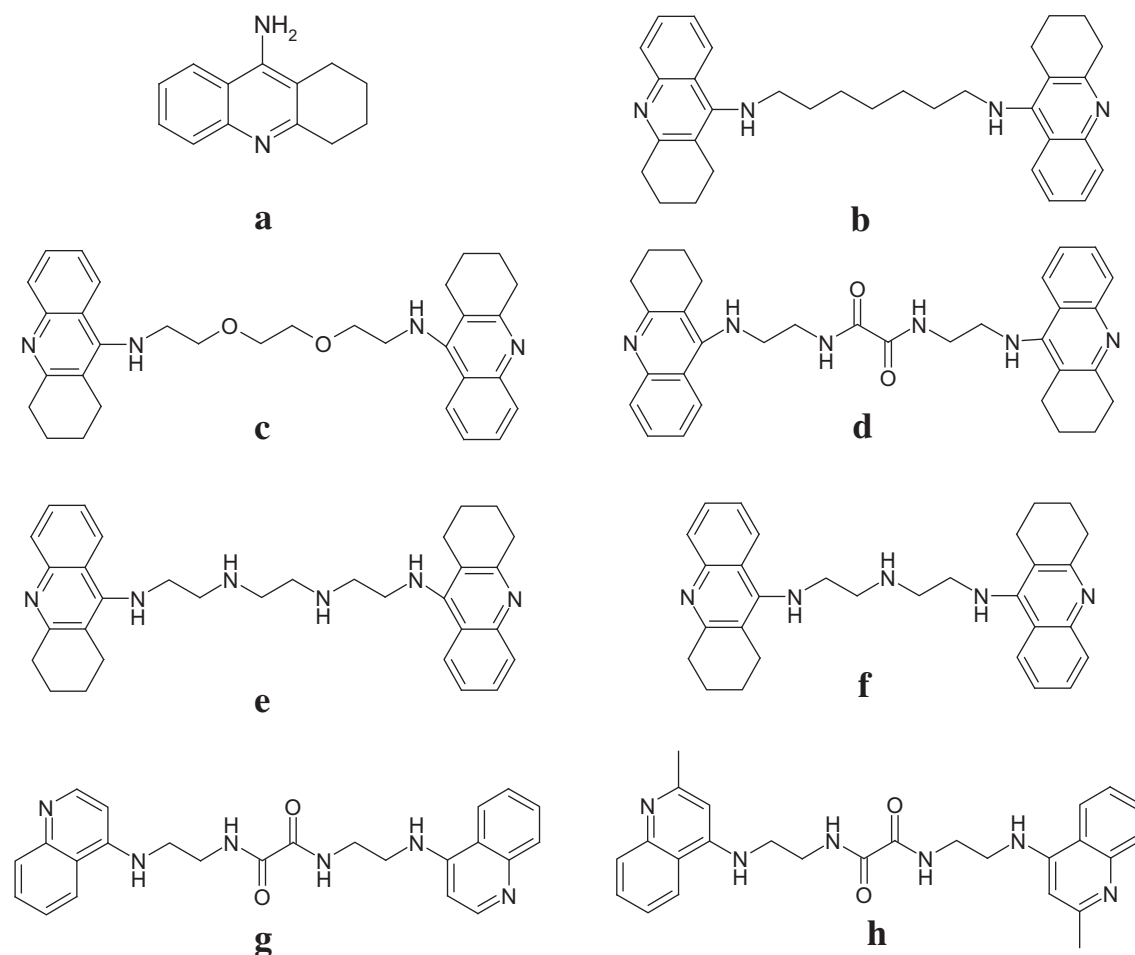
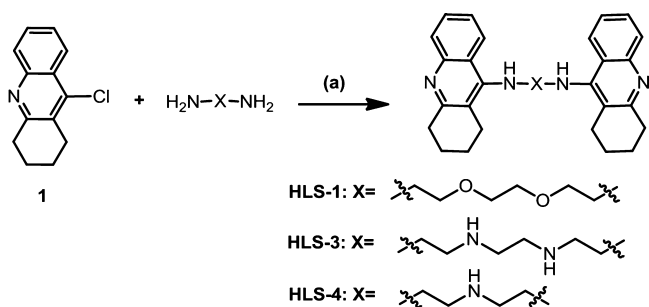


Fig. 1. Chemical structures of THA (a), B7T (b), HLS-1 (c), HLS-2 (d), HLS-3 (e), HLS-4 (f), HLS-5 (g) and HLS-6 (h).



**Scheme 1.** Reagents and conditions: (a) PhOH, NaI, 180 °C, 5 h (Bolognesi et al., 2007).

2010), however, most of studies only focused on how the anti-AChE activity was and whether the compounds have the potential of targeting other AD pathological factors described above. Few of them investigated the properties related to pharmaceuticals and biopharmaceutics, such as solubility (related to formulation development), cytotoxicity (related to safety of compounds) and the penetration capacity through intestinal epithelium into mesenteric vein or across blood–brain-barrier into brain (related to pharmacokinetics). In addition to pharmacological effect, both safety and pharmacokinetic aspects are also important factors in research and development of pharmaceuticals. In our study, based on the structure of B7T, modification of the linkage between two THA molecular fragments by inserting hydrogen donors and acceptors (*i.e.*, ether group, amide group and amine group) were designed in order to optimize their physicochemical properties, membrane permeability and hence pharmacokinetics. Among all synthesized compounds, HLS-3, HLS-4, HLS-5 and HLS-6 (Fig. 1) were novel designed, while HLS-1 and HLS-2 have been reported by Bolognesi et al. (Bolognesi et al., 2007). The present study aims to investigate *in vitro* cholinesterase inhibition and characterize biopharmaceutical properties (*i.e.*, physicochemical properties, cell cytotoxicity, *in vitro* intestinal permeabilities) of six synthesized THA dimers with THA and B7T serving as controls.

## 2. Materials and methods

### 2.1. Materials

Bis(7)-tacrine dihydrochloride (B7T) was provided by Prof. Yifan Han (Department of Applied Biology and Chemical Technology, Institute of Modern Chinese Medicine, The Hong Kong Polytechnic University, Hong Kong). Tacrine hydrochloride (THA) was purchased from Enzo Life Sciences Inc. (Farmingdale, NY, USA). Zolpidem (as internal standard), ethopropazine, BW284c51,

from USB Corporation (Cleveland, OH, USA). Sodium dihydrogen phosphate, sodium phosphate dibasic, triethylamine, formic acid were purchased from BDH (Poole, England). Acetonitrile (HPLC grade) and ethyl acetate were purchased from RCI Labscan (Bangkok, Thailand). All other reagents were of at least analytical grade and were used without further purification. Deionized water was prepared from Millipore water purification system (Millipore, Milford, USA).

### 2.2. Chemistry

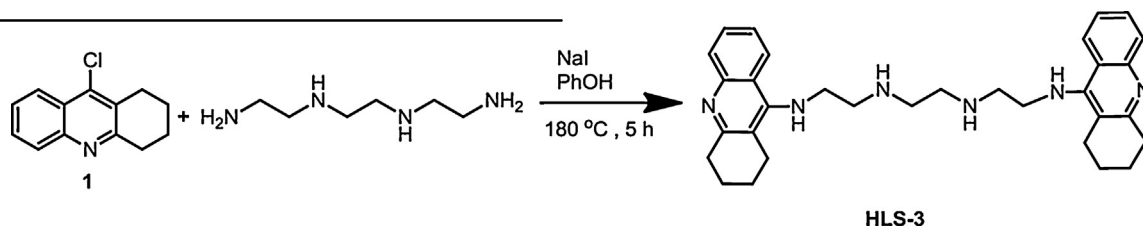
Reactions progress was monitored by TLC using EM Science silica gel 60 F254 plates. The developed chromatogram was analyzed by UV lamp (254 nm), ethanolic phosphomolybdic acid (PMA) or potassium permanganate (KMnO<sub>4</sub>). Liquid chromatography was performed using a forced flow (flash chromatography) of the indicated solvent system on Merck Silica Gel (230–400 mesh, 0.040–0.063 mm) using a coarse fritted glass column. <sup>1</sup>H and <sup>13</sup>C NMR spectra were recorded on Bruker spectrometers in CDCl<sub>3</sub>/DMSO-d<sub>6</sub>/D<sub>2</sub>O (400 MHz for <sup>1</sup>H and 100 MHz for <sup>13</sup>C). Chemical shifts in <sup>1</sup>H NMR spectra are reported in ppm on the δ scale from an internal standard of residual chloroform (7.27 ppm) or dimethyl sulfoxide (2.54 ppm) or D<sub>2</sub>O (4.79 ppm). Data are reported as follows: chemical shift, multiplicity (s=singlet, d=doublet, t=triplet, q=quartet, m= multiplet, br=broad), coupling constant in hertz (Hz), and integration. Chemical shifts of <sup>13</sup>C NMR spectra are reported in ppm from the central peak of CDCl<sub>3</sub> (77.16 ppm) or DMSO-d<sub>6</sub> (39.52 ppm) on the δ scale. High resolution mass spectra (HRMS) were obtained on a Finnigan MAT 95XL GC Mass Spectrometer by Miss. Ng Hau Yan of the Chinese University of Hong Kong, Department of Chemistry.

General Synthetic Schemes for Novel THA dimers were shown in Schemes 1 and 2.

9-Chloro-1,2,3,4-tetrahydroacridine (**1**), 9-[10-(1,2,3,4-tetrahydroacridin-9-yl)-4,7-dioxo-1,10-diazadecan-1-yl]-1,2,3,4-tetrahydroacridine (HLS-1) and *N,N'*-bis({2-[(1,2,3,4-tetrahydroacridin-9-yl) amino]ethyl}) ethanediamide (HLS-2) were first reported by Bolognesi et al. and synthesized according to their reported methods (Bolognesi et al., 2007).

9-[10-(1,2,3,4-Tetrahydroacridin-9-yl)-1,4,7,10-tetraazadecan-1-yl]-1,2,3,4-tetrahydroacridine (HLS-3), *N*-[2-({2-[(1,2,3,4-tetrahydroacridin-9-yl) amino]ethyl}) amino] ethyl]-1,2,3,4-tetrahydroacridin-9-amine (HLS-4), *N,N'*-bis({2-[(quinolin-4-yl) amino]ethyl}) ethanediamide (HLS-5) and *N,N'*-bis({2-[(2-methylquinolin-4-yl) amino]ethyl}) ethanediamide (HLS-6) were new compounds, and were prepared according to the general synthetic schemes shown below.

#### 2.2.1. 9-[10-(1,2,3,4-Tetrahydroacridin-9-yl)-1,4,7,10-tetraazadecan-1-yl]-1,2,3,4-tetrahydroacridine (HLS-3)

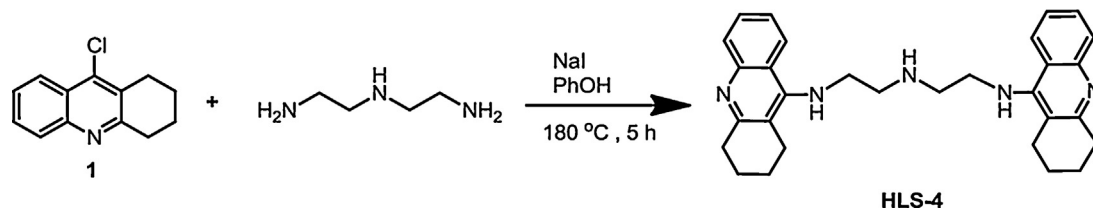


acetylcholine iodide, *S*-butyrylthiocholine iodide, and 5,5'-dithio-bis (2-nitrobenzoic acid) (DTNB) were purchased from Sigma (St. Louis, MO, USA). Sodium dodecyl sulphate (SDS) was purchased

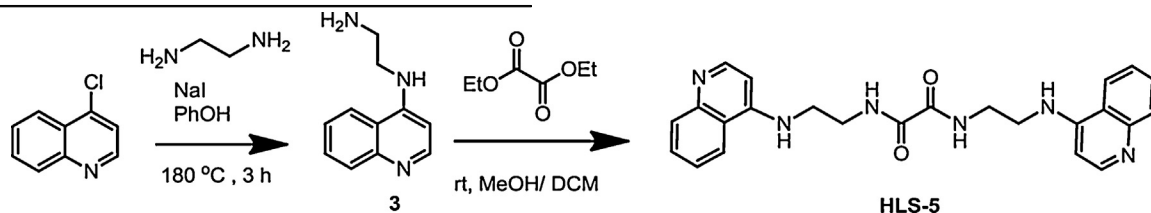
A mixture of **1** (0.74 g, 3.4 mmol), triethylenetetramine (0.25 g, 1.7 mmol), phenol (1.80 g, 19 mmol), and NaI (0.10 g, 0.67 mmol) was heated at 180 °C under nitrogen for 5 h and then cooled to

room temperature. The mixture was diluted with  $\text{CH}_2\text{Cl}_2$  and made basic with 10% KOH solution. The organic layer was washed with water and brine and dried with  $\text{Na}_2\text{SO}_4$ . Solvent was removed under vacuum and the resulting residue was washed with  $\text{Et}_2\text{O}$  and further purified by flash-chromatography ( $\text{CH}_2\text{Cl}_2/\text{MeOH}/\text{aqueous } 28\% \text{ ammonia} = 7.5:2.5:0.05$ ) to give HLS-3 (0.48 g, 56%).  $^1\text{H NMR}$  (400 MHz,  $\text{CDCl}_3$ )  $\delta$ : 8.03–7.97 (m,  $^2\text{H}$ ), 7.92–7.89 (m,  $^2\text{H}$ ), 7.56–7.49 (m,  $^2\text{H}$ ), 7.32–7.28 (m,  $^2\text{H}$ ), 4.98 (brs,  $^2\text{H}$ ), 3.58–3.50 (m,  $^4\text{H}$ ), 3.05–2.98 (m,  $^4\text{H}$ ), 2.93–2.82 (m,  $^4\text{H}$ ), 2.78–2.54 (m,  $^8\text{H}$ ), 1.87–1.84 (m,  $^{10}\text{H}$ ).  $^{13}\text{C NMR}$  (100 MHz,  $\text{CDCl}_3$ )  $\delta$ : 158.3, 151.0, 147.2, 128.4, 128.3, 123.6, 122.8, 120.2, 116.0, 49.8, 49.0, 48.2, 33.8, 24.9, 23.0, 22.8. HRMS-ESI ( $m/z$ ):  $[\text{M} + \text{H}]^+$  calculated for  $\text{C}_{32}\text{H}_{41}\text{N}_6$ : 509.3393; found 509.3395.

#### 2.2.2. N-[2-({2-[(1,2,3,4-Tetrahydroacridin-9-yl) amino]ethyl}amino)ethyl]-1,2,3,4-tetrahydroacridin-9-amine (HLS-4)



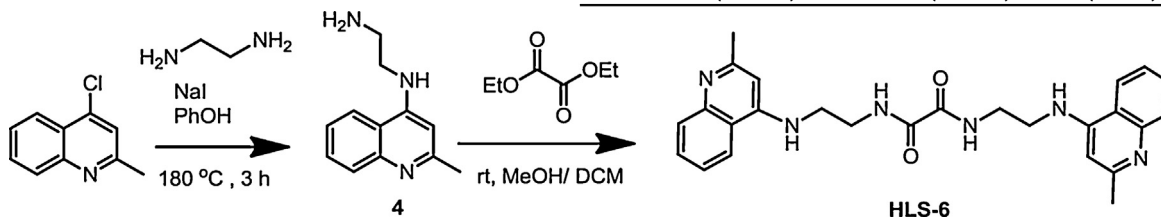
It was obtained from **1** (0.74 g, 3.4 mmol) and diethylenetriamine (0.18 g, 1.7 mmol) by following the procedure analogous to



that described for HLS-3 and purified by flash-chromatography ( $\text{CH}_2\text{Cl}_2/\text{MeOH}/\text{aqueous } 28\% \text{ ammonia} = 8:2:0.05$ ) to give HLS-4 (0.34 g, 43%).

$^1\text{H NMR}$  (400 MHz,  $\text{CDCl}_3$ )  $\delta$ : 8.00 (d,  $J = 8.3 \text{ Hz}$ ,  $^2\text{H}$ ), 7.91 (d,  $J = 8.3 \text{ Hz}$ ,  $^2\text{H}$ ), 7.54 (t,  $J = 7.4 \text{ Hz}$ ,  $^2\text{H}$ ), 7.32 (t,  $J = 7.4 \text{ Hz}$ ,  $^2\text{H}$ ), 4.68 (brs,  $^2\text{H}$ ), 3.58–3.50 (m,  $^4\text{H}$ ), 3.07–3.04 (m,  $^4\text{H}$ ), 2.94–2.92 (m,  $^4\text{H}$ ), 2.77–2.74 (m,  $^4\text{H}$ ), 1.89 (brs,  $^8\text{H}$ ), 1.37 (brs,  $^1\text{H}$ ).  $^{13}\text{C NMR}$  (100 MHz,  $\text{CDCl}_3$ )  $\delta$ : 158.8, 150.7, 147.7, 129.0, 128.4, 123.9, 122.7, 120.6, 116.6, 50.0, 48.7, 34.2, 25.1, 23.2, 22.9. HRMS-ESI ( $m/z$ ):  $[\text{M} + \text{H}]^+$  calculated for  $\text{C}_{30}\text{H}_{36}\text{N}_5$ : 466.2971; found 466.2966.

#### 2.2.3. N,N'-Bis[2-((quinolin-4-yl) amino)ethyl] ethanediamide (HLS-5)



**3** (0.20 g) was obtained by following the preparation procedure of **2** from the commercially available 4-chloroquinoline and 1,2-diaminoethane in 85% yield.  $^1\text{H NMR}$  (400 MHz,  $\text{CDCl}_3$ )  $\delta$ : 8.56 (d,  $J = 5.2 \text{ Hz}$ ,  $^1\text{H}$ ), 7.97 (d,  $J = 8.4 \text{ Hz}$ ,  $^1\text{H}$ ), 7.81 (d,  $J = 8.3 \text{ Hz}$ ,  $^1\text{H}$ ), 7.61 (t,

$J = 7.2 \text{ Hz}$ ,  $^1\text{H}$ ), 7.42 (t,  $J = 7.2 \text{ Hz}$ ,  $^1\text{H}$ ), 6.42 (d,  $J = 5.2 \text{ Hz}$ ,  $^1\text{H}$ ), 5.76 (brs,  $^1\text{H}$ ), 3.37–3.33 (m,  $^2\text{H}$ ), 3.13–3.10 (m,  $^2\text{H}$ ), 1.46 (brs,  $^2\text{H}$ ).  $^{13}\text{C NMR}$  (100 MHz,  $\text{CDCl}_3$ )  $\delta$ : 151.2, 150.0, 148.6, 130.0, 129.1, 124.7, 119.7, 119.1, 99.1, 45.0, 40.6.

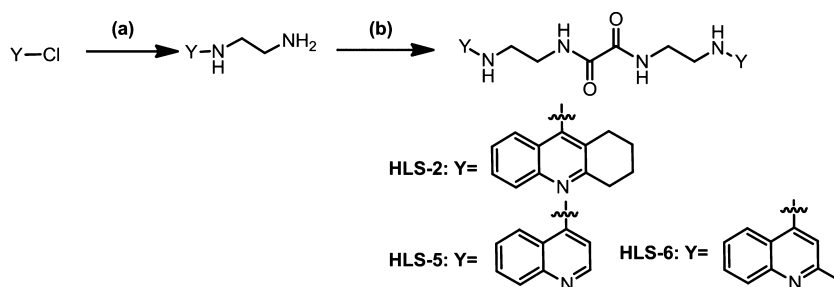
A solution of **3** (0.19 g, 1.0 mmol) and diethyloxalate (63 mg, 0.5 mmol) in  $\text{MeOH}/\text{CH}_2\text{Cl}_2$  (1:2) 24 ml was stirred at room temperature for 24 h. Solvent was removed under vacuum and the resulting residue was purified by flash-chromatography ( $\text{CH}_2\text{Cl}_2/\text{MeOH}/\text{aqueous } 28\% \text{ ammonia} = 7.5:2.5:0.05$ ) to give HLS-5 (0.12 g, 58%).  $^1\text{H NMR}$  (400 MHz,  $\text{D}_2\text{O}$ )  $\delta$ : 8.08 (d,  $J = 6.9 \text{ Hz}$ ,  $^2\text{H}$ ), 7.91 (d,  $J = 8.3 \text{ Hz}$ ,  $^1\text{H}$ ), 7.77 (t,  $J = 7.6 \text{ Hz}$ ,  $^1\text{H}$ ), 7.60–7.55 (m,  $^2\text{H}$ ), 7.53–7.49 (m,  $^2\text{H}$ ), 7.34–7.32 (m,  $^1\text{H}$ ), 7.25–7.23 (m,  $^1\text{H}$ ), 6.60 (brs,  $^2\text{H}$ ), 3.69 (brs,  $^4\text{H}$ ), 3.64 (brs,  $^4\text{H}$ ).  $^{13}\text{C NMR}$  (100 MHz,  $\text{DMSO}-d_6$ )  $\delta$ : 160.6, 156.0, 142.9, 138.3, 133.8, 127.0, 123.3, 120.7, 117.1, 98.4, 42.5, 37.6. HRMS-ESI ( $m/z$ ):  $[\text{M} + \text{H}]^+$  calculated for  $\text{C}_{24}\text{H}_{25}\text{N}_6\text{O}_2$ : 429.2034; found 429.2035.

#### 2.2.4. N,N'-Bis[2-((2-methylquinolin-4-yl) amino)ethyl] ethanediamide (HLS-6)

**4** (0.23 g) was obtained by following the preparation procedure of **2** from the commercially available 4-chloroquinoline and 1,2-diaminoethane in 85% yield.  $^1\text{H NMR}$  (400 MHz,  $\text{CDCl}_3$ )  $\delta$ : 7.89 (d,  $J = 8.3 \text{ Hz}$ ,  $^1\text{H}$ ), 7.78 (d,  $J = 8.3 \text{ Hz}$ ,  $^1\text{H}$ ), 7.55 (t,  $J = 7.5 \text{ Hz}$ ,  $^1\text{H}$ ), 7.30 (t,  $J = 7.5 \text{ Hz}$ ,  $^1\text{H}$ ), 6.28 (s,  $^1\text{H}$ ), 5.89 (brs,  $^1\text{H}$ ), 3.24 (brs,  $^2\text{H}$ ), 3.02–2.99 (m,  $^2\text{H}$ ), 2.59 (s,  $^3\text{H}$ ), 1.46 (brs,  $^1\text{H}$ ).  $^{13}\text{C NMR}$  (100 MHz,  $\text{CDCl}_3$ )  $\delta$ : 159.4, 149.9, 148.1, 128.9, 128.7, 123.7, 119.6, 117.5, 99.0, 44.9, 40.2, 25.6.

HLS-6 (0.13 g) was obtained by following an analogous procedure described for HLS-5 in 55% yield.  $^1\text{H NMR}$  (400 MHz,  $\text{CDCl}_3$ )  $\delta$ : 7.90 (d,  $J = 8.3 \text{ Hz}$ ,  $^2\text{H}$ ), 7.69 (d,  $J = 8.1 \text{ Hz}$ ,  $^2\text{H}$ ), 7.60 (t,  $J = 7.3 \text{ Hz}$ ,  $^2\text{H}$ ), 7.36 (t,  $J = 7.3 \text{ Hz}$ ,  $^2\text{H}$ ), 6.27 (s,  $^2\text{H}$ ), 5.82 (brs,  $^2\text{H}$ ), 3.81–3.76 (m,  $^4\text{H}$ ), 3.53–3.49 (m,  $^6\text{H}$ ), 2.61 (s,  $^6\text{H}$ ).  $^{13}\text{C NMR}$

(100 MHz,  $\text{DMSO}-d_6$ )  $\delta$ : 160.6, 155.5, 155.4, 154.9, 154.3, 138.4, 138.3, 133.6, 126.4, 126.4, 123.7, 123.2, 120.1, 120.0, 116.2, 116.0, 98.9, 98.7, 46.0, 42.3, 40.7, 37.6, 37.5, 20.4, 20.3. HRMS-ESI ( $m/z$ ):  $[\text{M} + \text{H}]^+$  calculated for  $\text{C}_{26}\text{H}_{29}\text{N}_6\text{O}_2$ : 457.2347; found 457.2346.



**Scheme 2.** Reagents and conditions: (a)  $\text{NH}_2\text{CH}_2\text{CH}_2\text{NH}_2$ , PhOH, NaI,  $180^\circ\text{C}$ , 3 h; (b) diethyl oxalate,  $\text{CHCl}_3$  or  $\text{MeOH}/\text{CH}_2\text{Cl}_2$ , room temperature, 24 h (Bolognesi et al., 2007).

### 2.3. In silico prediction of Log P, solubility and $\text{pK}_a$ for THA dimers

Log P values (octanol–water partition coefficient), aqueous solubility and  $\text{pK}_a$ s for all the tested THA dimers were calculated by the ACD/Labs online program (<http://ilab.acdlabs.com/iLab2/>, Toronto, Canada). For the neutral form of a molecule, the error of the calculated Log P is within 0.3 Log P unit or better in most cases by ACD/Labs program (Malík et al., 2007). Structures (unionized form) were entered as SMILES notation.

### 2.4. Inhibition of the tested THA dimers on cholinesterases and related mechanisms

The cholinesterase assay was performed using a colorimetric method reported by Ellman et al. with minor modification (Ellman et al., 1961; Padilla et al., 1999). Individual stock solution ( $\sim 10$  mM) of the test compounds (HLS-1, HLS-2, HLS-3, HLS-4, HLS-5, HLS-6, B7T and THA) was prepared in DMSO. Appropriate amount of stock solution was further diluted with water to yield working solutions with at least nine different concentrations (in the range of  $\sim 10^{-4}$  to  $10^{-10}$  M). The frozen stocked rat cortex homogenate (AChE source) was thawed at  $4^\circ\text{C}$  in water bath and further diluted with 5 volume (v/v) ice-cold phosphate buffer solution (PBS, 0.1 M, pH 7.5) to yield the rat cortex homogenate. Frozen rat serum was also thawed without further dilution.

To study *in vitro* inhibition effect on AChE/BChE, 0.1 ml of cortex homogenate/serum was pre-incubated for 5 min in 1.7 ml PBS 7.5 containing with ethopropazine (0.1 mM)/BW284c51 (0.01 mM), which were the selective inhibitors of BChE/AChE, respectively. Then, 0.1 ml of working solution of tested compound was added and followed by pre-incubation for 5 min. The reaction was initiated by addition of 0.1 ml of acetylcholine iodide (20 mM)/S-butrylthiocholine iodide (60 mM), substrate of AChE/BChE, respectively. After incubation at  $37^\circ\text{C}$  in water bath for 30 min, the reaction was terminated by 1 ml of 3% (w/v) SDS followed by 1 ml of 0.2% (w/v) DTNB (chromogenic reagent) to yield a yellow anion of 5-thio-2-nitro-benzoic acid. The extent of color production was measured spectrophotometrically at 415 nm using microplate reader (Benchmark<sup>TM</sup>; Bio-Rad Tokyo, Japan). For the reference control, 0.1 ml of water was replaced with the test compound solution. For blank control, additional 0.1 ml of water was instead of cholinesterase sources. The enzyme activity was expressed as a percentage of the activity observed in tested sample relative to that from the reference control.

To verify the inhibition types of THA dimers on AChE, the enzyme reaction assay was carried out in presence of inhibitor and substrate at various concentrations. The Michaelis constant ( $K_m$ ) of AChE was determined in initial experiment by using different concentrations of substrate (acetylcholine iodide). After pre-incubation of AChE source with ethopropazine (0.1 mM) and each test compound at three concentrations for 5 min, the enzyme reaction was initiated by addition of the appropriate substrate at

five concentrations close to the predetermined  $K_m$ . The reaction was terminated at 15 min by adding 3% SDS, the absorbance of the generated yellow complex from DTNB was measured as described above.

### 2.5. Content analyses of THA and its dimers for bidirectional transport study

#### 2.5.1. HPLC-UV assay for THA, HLS-1, HLS-2 and B7T

The individual analysis of THA, HLS-1, HLS-2 and B7T were carried out using HPLC-UV method. The HPLC-UV system consists of Waters 600 controller (pump), Waters 717 auto sampler and Waters 996 Photodiode Array detector. Data collection was performed using a Waters Millennium Chromatography Manager data system (Version 3.20). Chromatographic separation was achieved by a Thermo BDS Hypersil  $\text{C}_{18}$  analytical column ( $250 \times 4.6$  mm,  $5 \mu\text{m}$ ) protected by a guard column (Delta-Pak<sup>TM</sup>  $\text{C}_{18}$  Guard-Pak Waters). Mobile phase consisted of eluent A (50 mM sodium dihydrogen phosphate and 0.5% (v/v) triethylamine (adjusted to pH 3.0 by  $\text{H}_3\text{PO}_4$ ) with 5% acetonitrile) and eluent B (acetonitrile). The HPLC column was isocratically eluted by a mixture of eluent A: eluent B (2:8 (v/v) for THA, HLS-1 and HLS-2; 3:7 (v/v) for B7T) at a flow rate of 1 ml/min. UV detection was performed at a wavelength of 241 nm for THA and 245 nm for studied THA dimers. The temperatures of column and autosampler were set at ambient and  $4^\circ\text{C}$ , respectively. The sample injection volume was 50  $\mu\text{l}$ .

#### 2.5.2. LC-MS/MS assay for HLS-3, and HLS-4

The individual analysis of HLS-3 and HLS-4 were carried out using LC-MS/MS method. The LC-MS/MS system, consisted of an Agilent 6430 triple quadrupole mass spectrometer equipped with an electrospray ionization source (ESI), two Agilent 1290 series pumps and autosampler (Agilent Technologies, Inc., CA, USA), was used to perform the analysis. Data were acquired and analyzed using Agilent MassHunter Quantitative Analysis B.03.01 software. The chromatographic separation was achieved by using an Agilent ZORBAX Eclipse XDB  $\text{C}_{18}$  column ( $150 \times 2.1$  mm,  $3.5 \mu\text{m}$ ) which was protected by a pre-column filter. The HPLC column was eluted by a mixture of 0.1% formic acid in water and acetonitrile (65:35, v/v) at a flow rate of 0.25 ml/min. The temperatures of column and autosampler were set at ambient and  $6^\circ\text{C}$ , respectively. The sample injection volume was 10  $\mu\text{l}$ .

The mass spectrometer was operated at positive ionization mode. The LC elute was sprayed into the mass spectrometer at a desolvation gas temperature of  $350^\circ\text{C}$  and at a spray voltage of +4.0 kV. Nitrogen was used as both desolvation (8 l/min) and nebulizer gas (30 psi). With the aid of Mass Hunter Optimizer software (Version B.03.01), the mass spectrometer was optimized prior to the analysis by post column infusion of 1  $\mu\text{g}/\text{ml}$  of analytes with a LC flow at 0.15 ml/min flow rate. Data acquisition was conducted at multiple reaction monitoring (MRM) with optimized

parameters for each analyte. The Dwell time for each MRM transition was set at 150 ms. The LC eluent was discarded 0.25 min prior to the first peak into the waste bottle by divert valve.

## 2.6. Evaluation of cytotoxicity, intestinal permeability of THA dimers by Caco-2 cell model

### 2.6.1. Cell culture

For cell culture, Caco-2 cells were cultured in DMEM supplemented with 10% of FBS at 37 °C as we described before (Zhang et al., 2007). For cytotoxicity study, Caco-2 cells were seeded onto the 96-well plates in DMEM cultural medium at the density of  $5 \times 10^4$  cells/well and cultured at 37 °C for 24 h in incubation chamber. For transport study, Caco-2 cells were seeded onto the apical surface of 6-well plates Transwell® inserts at a density of  $3 \times 10^5$  cells/well and cultured for 21 days prior to transport experiments. Caco-2 cells from passage 38–47 and monolayers with TEER above  $600 \Omega \text{cm}^2$  (measured by EVOM-G, World Precision Instruments, Inc., Sarasota, FL, USA) were employed in the transport studies.

### 2.6.2. Cytotoxicity study

The *in vitro* cytotoxicity of THA dimers on Caco-2 cells was evaluated by MTT assay (Jeong and Choi, 2007). PBS<sup>+</sup> was used in this study and prepared by dissolving a phosphate-buffered saline tablet in 200 ml of deionized water, followed by addition of 90  $\mu\text{l}$  of 2 M calcium chloride and 80  $\mu\text{l}$  of 1 M magnesium chloride, pH value was adjusted to 6.8 by  $\text{H}_3\text{PO}_4$  (Ng et al., 2005). After incubation for 24 h, the cultural medium was replaced by 150  $\mu\text{l}$  of PBS<sup>+</sup> containing test compound at a series of concentrations (in the range of  $\sim 10^{-6}$  to  $10^{-3}$  M). The blank PBS<sup>+</sup> was used as negative control. After incubation for 4 h (at 37 °C, 5%  $\text{CO}_2$ ), samples were removed and MTT reagent dissolved in PBS<sup>+</sup> was subsequently applied to each well, then the plate was incubated at 37 °C for another 2 h. Finally, the solution in each well was removed and 200  $\mu\text{l}$  of DMSO was added to dissolve the purple formazan product (reduced from MTT by living cells (Mosmann, 1983)). The wells containing 200  $\mu\text{l}$  of DMSO were served as blank. Absorbance of the solution in each well was measured at 595 nm ( $\text{OD}_{595}$ ) by a Kinetic microplate reader (Benchmark™, Bio-Rad Tokyo, Japan).

### 2.6.3. Bidirectional transport study

The transport study was carried out bidirectionally in PBS<sup>+</sup> 6.8 as we described before (Li et al., 2012). Briefly, THA and its dimers at different concentrations in PBS<sup>+</sup> were loaded onto the apical side (AP, 1.5 ml of transport buffer) or basolateral side (BL, 2.6 ml of transport buffer), the so-called donor chamber. Aliquots of 0.5 ml samples were collected from the other side, namely the receiver

chamber, at different time intervals (15, 30, 45, 60 and 90 min for THA; 30, 60, 90, 120 and 150 min for THA dimers) during the experiment. Same volume of blank PBS<sup>+</sup> was immediately added to the receiver chamber after each sampling in order to maintain a constant volume. Samples taken from the transport studies were mixed with 0.1 ml of acetonitrile, and stored at  $-80^\circ\text{C}$  until analyses.

In addition to determination of the permeabilities of the tested THA dimers, the intracellular amounts of tested compounds were also measured to estimate the extent of cell uptake of the compounds during the absorption process. After the transport studies, the Caco-2 cell monolayers were rinsed twice with ice-cold saline and collected from Transwell® inserts by surgical scissors at the end of transport studies. The tested compounds were extracted from the obtained monolayers by sonication for 10 min with 1.5 ml of acetonitrile. After centrifugation at  $16,000 \times g$  for 5 min, the collected supernatant was then evaporated to dryness under a gentle stream of nitrogen at 37 °C. The obtained residue was reconstituted with the corresponding mobile phase and analyzed.

## 2.7. Data analyses

### 2.7.1. Calculation of relative cell viability in cytotoxicity test

The relative cell viability (%) was calculated based on following equation as described previously (Yang et al., 2012).

$$\text{Relative cell activity (\%)} = \frac{\text{OD}_{595, \text{sample}} - \text{OD}_{595, \text{blank}}}{\text{OD}_{595, \text{control}} - \text{OD}_{595, \text{blank}}} \times 100\%$$

where “ $\text{OD}_{595, \text{sample}}$ ” is the average absorbance of the sample treated Caco-2 cells, “ $\text{OD}_{595, \text{control}}$ ” is the average absorbance of the control cells, and “ $\text{OD}_{595, \text{blank}}$ ” is the average absorbance of 200  $\mu\text{l}$  DMSO in well at 595 nm. Cytotoxicity results of THA dimers was expressed as 50% lethal concentrations ( $\text{LC}_{50}$ ), calculated by the probit method (Finney, 1971) with help of GraphPad Prism software version 5.0.

### 2.7.2. Calculation of permeability coefficient in Caco-2 cell model

The permeability coefficient ( $P_{\text{app}}$ ) was calculated by the equation described previously (Li et al., 2012).

$$P_{\text{app}} = \frac{dC/dt \times V}{A \times C}$$

where “ $dC/dt$ ” is the change of the compound concentration in receiver chamber over time, “ $V$ ” represents the volume of the solution in receiver chamber ( $\text{cm}^3$ ), “ $A$ ” is the membrane surface

**Table 1**

*In silico* prediction of Log  $P$ ,  $pK_a$ , aqueous solubilities at different pH and the number of hydrogen bond donors and acceptors for THA and its novel dimers.

Compounds	MW	NHD	NHA	Log $P$	$S_{\text{water}}^a$	$pK_a$	Aqueous solubilities at different pH (mg/ml)				
							pH 1.7 (Stomach)	pH 4.6 (Duodenum)	pH 6.5 (Jejunum)	pH 7.4 (Ileum)	pH 8 (Colon)
THA	198.3	2	2	2.6 (2.4) <sup>b</sup>	36	$9.9 \pm 0.4$ ( $9.9 \pm 0.2$ ) <sup>b</sup>	34.45	34.45	28	12.22	4.24
HLS-1	510.7	2	6	5.7	0.0043	$pK_{a1}: 9.7 \pm 0.4$ , $pK_{a2}: 10.3 \pm 0.4$	0.18	0.18	0.16	0.04	<0.01
HLS-2	536.7	4	8	4.4	0.012	$pK_{a1}: 9.6 \pm 0.4$ , $pK_{a2}: 10.2 \pm 0.4$	0.06	0.06	0.05	0.01	<0.01
HLS-3	508.7	4	6	5.3	0.100	$pK_{a1}: 7.3 \pm 0.5$ , $pK_{a2}: 9.4 \pm 0.4$ , $pK_{a3}: 10.3 \pm 0.4$	313.7	193.4	29.95	4.13	0.14
HLS-4	465.7	3	5	5.6	0.17	$pK_{a1}: 7.9 \pm 0.5$ , $pK_{a2}: 9.7 \pm 0.4$ , $pK_{a3}: 10.3 \pm 0.4$	8.28	8.28	5.11	0.22	0.01
HLS-5	428.5	4	8	2.8	0.011	$pK_{a1}: 8.6 \pm 0.4$ , $pK_{a2}: 9.2 \pm 0.4$	2.64	2.58	0.63	0.07	<0.01
HLS-6	456.5	4	8	3.6	0.004	$pK_{a1}: 9.0 \pm 0.4$ , $pK_{a2}: 9.6 \pm 0.4$	0.83	0.83	0.22	0.01	<0.01
B7T	492.7	2	4	7.8 (8.2) <sup>b</sup>	0.00032	$pK_{a1}: 8.6 \pm 0.4$ , $pK_{a2}: 10.2 \pm 0.4$ ( $pK_{a1}: 8.7 \pm 0.1$ ) <sup>b</sup> ( $pK_{a2}: 10.7 \pm 0.4$ ) <sup>b</sup>	<0.01	<0.01	<0.01	<0.01	<0.01

<sup>a</sup>  $S_{\text{water}}$ : water solubility, unit =  $\mu\text{g/ml}$ .

<sup>b</sup> Experimental data from reference (Yu et al., 2008).

area (cm<sup>2</sup>). “C” is the initial compound concentration in the donor chamber.

The recoveries of studied compounds from the two cell monolayer models were calculated using following equation (Zhang et al., 2008):

$$\text{Recovery}(\%) = \frac{A_{\text{apical}} + A_{\text{basolateral}}}{A_0} \times 100\%$$

where  $A_0$  is the initial amount of the loading compound,  $A_{\text{apical}}$  is the amount of the compound in apical chamber at the end of the transport studies, and  $A_{\text{basolateral}}$  is the cumulative amount of the compound permeated to the basolateral chamber at the end of the transport studies.

In addition, the efflux ratio was calculated by the following equation to assess the extent of drug efflux (Balimane et al., 2006) on Caco-2 cell model.

$$\text{Efflux ratio} = \frac{P_{\text{app(B} \rightarrow \text{A)}}}{P_{\text{app(A} \rightarrow \text{B)}}$$

where “ $P_{\text{app(B} \rightarrow \text{A)}}$ ” and “ $P_{\text{app(A} \rightarrow \text{B)}}$ ” are the mean of  $P_{\text{app}}$  values from the basolateral to apical (secretive) and apical to basolateral (absorptive) direction, respectively.

### 2.7.3. Statistical analysis

Statistical analysis was performed using a statistical software package SPSS (version 17, SPSS Inc., Chicago, IL, USA). One-way ANOVA with multiple comparisons of the means was applied for analysis of the data from transport studies. A probability level of  $p < 0.05$  was set as the criterion of significance.

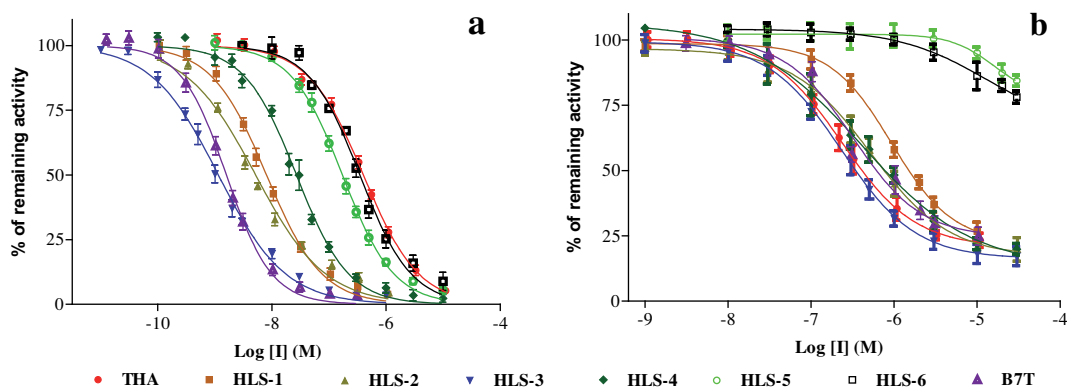
## 3. Results

### 3.1. In silico prediction of Log P, solubility and pK<sub>a</sub> of the THA dimers

The *n*-octanol–water partition coefficient is the ratio of equilibrated compound concentrations in *n*-octanol versus that in water at a specified temperature (typically 25 °C). Partition coefficient, commonly represented as Log *P*, is a good surrogate for evaluating the partitioning ability of chemicals through lipid membranes, and considered to be one of the most important physicochemical descriptor to predict the *in vitro* and *in vivo* permeability across biological membranes (Nakao et al., 2009). In addition to Log *P*, water solubility, aqueous solubilities as a function of pH and pK<sub>a</sub> are also related to compound permeability, dissolution rate and its formulation strategy. Table 1 summarized the molecular weight (MW), the number of hydrogen bond donors (NHD) and acceptors (NHA) and predicted physicochemical properties of THA and its THA dimers. It is noticed that the current predicted values on Log *P* and pK<sub>a</sub> of THA and B7T were quite comparable to that obtained from previously reported experimental values (Yu et al., 2008).

After adding different linkers between two THA molecules, the MW of THA dimers was close to 500, which was at the borderline of Lipinski's rule of five (Lipinski et al., 2001). The NHD and NHA of THA dimers were within 5 and 10, respectively. Among the studied THA dimers, B7T had the highest Log *P* value (7.8), followed by HLS-1, HLS-4, HLS-3, HLS-2, HLS-6 and HLS-5. Water solubilities of THA dimers (in the range of 0.00032–0.17 μg/ml) were generally very poor with HLS-3 and HLS-4 showed relatively higher solubilities than that of the other THA dimers.

Since the ionizable groups in THA dimers structures were mainly amine group or amide group, THA dimers demonstrated to



Compound	IC <sub>50</sub> (nM)		Selectivity index <sup>a</sup>	AChE inhibition constant (nM)		Inhibition type
	AChE	BChE		K <sub>i</sub>	K' <sub>i</sub>	
THA	365 ± 35	228.5 ± 38.8	0.63	355.5	473.5	mixed
HLS-1	7.8 ± 0.7	1014.0 ± 177.5	130	4.9	12.3	mixed
HLS-2	3.8 ± 0.3	511.5 ± 74.0	135	2.1	3.1	mixed
HLS-3	1.1 ± 0.1	234.3 ± 25.2	213	0.9	1.3	mixed
HLS-4	28.0 ± 2.3	398.1 ± 67.7	14.2	25.0	36.7	mixed
HLS-5	146.1 ± 16.9	N.D.	N.A.	N.A.	N.A.	N.A.
HLS-6	244.6 ± 28.5	N.D.	N.A.	N.A.	N.A.	N.A.
B7T	1.5 ± 0.2	328.9 ± 43.5	219	1.1	1.4	mixed

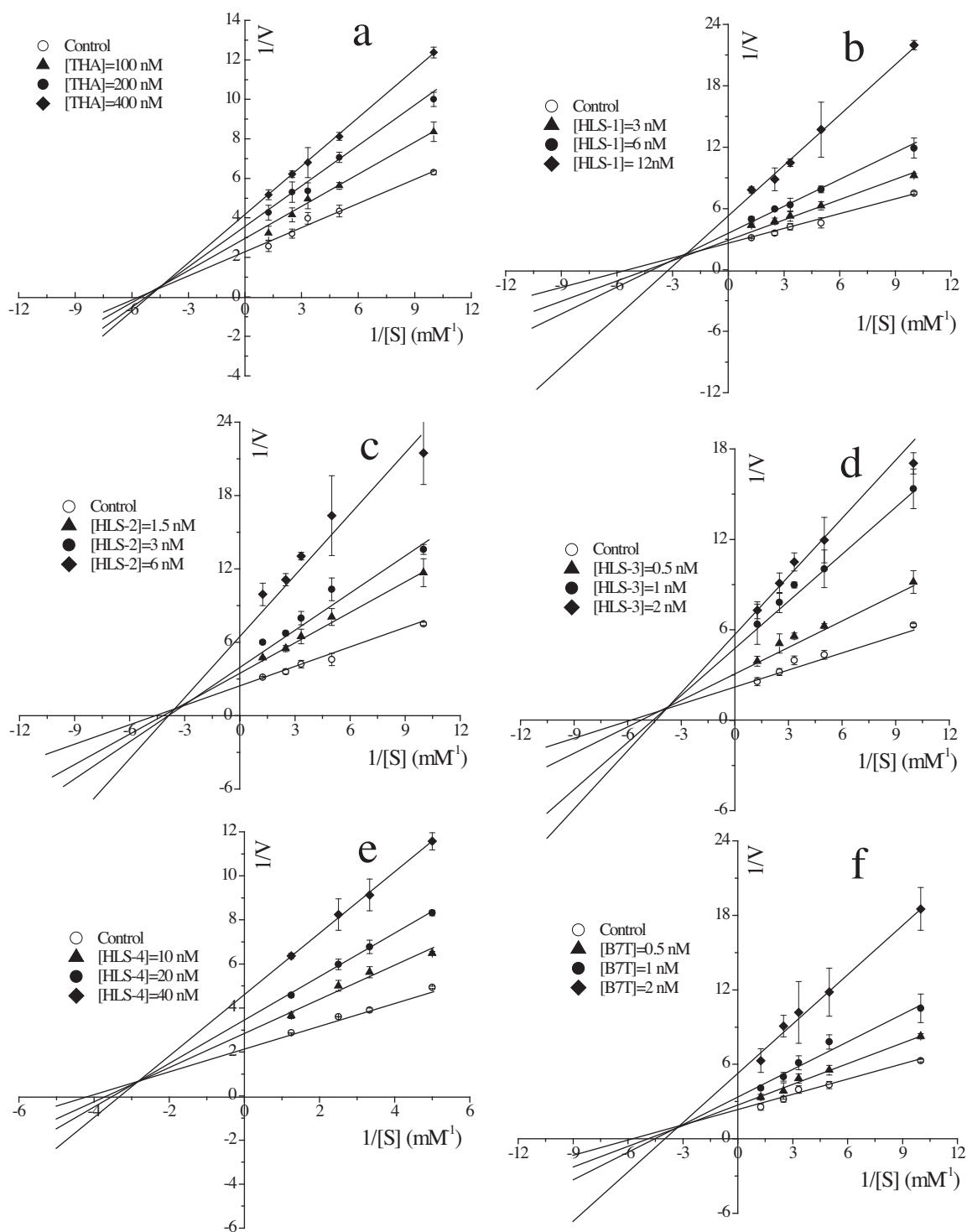
<sup>a</sup>: selectivity index = IC<sub>50</sub>(BChE)/IC<sub>50</sub>(AChE); N.D.: not detectable; N.A.: not applicable

Fig. 2. Dose-response curves of tested novel THA dimers on inhibition of AChE (a) and BChE (b). Each point represents mean ± s.d. (n=5).

be basic compounds. The predicted  $pK_a$  values for all THA dimers were higher than 7.3 with highest  $pK_{a2}$  of 10.7 after second ionization. Theoretically, according to the intrinsic solubility ( $S_0$ ) of a basic compound and its  $pK_a$  value, the apparent solubility ( $S$ ) at a specific pH condition could be estimate from the following equation (Guo and Shen, 2004):

$$S = S_0(1 + 10^{pK_a - pH})$$

When  $pH > pK_a$ , the apparent solubility  $S$  would be close to its intrinsic solubility  $S_0$  of basic compound. When  $pH < pK_a$ ,  $S$  would be higher than  $S_0$  and geometrically increase with the decrease of pH. Based on the predicted  $pK_a$  values of the studied THA dimers, acidic condition rather than neutral and basic condition would facilitate their dissolving processes. The predicted aqueous solubilities of THA and its dimers under various physiological conditions are also summarized in Table 1. Among all studied



**Fig. 3.** Lineweaver–Burk plots for inhibition of rat cortex AChE by THA (a) and its dimers (HLS-1 (b), HLS-2 (c), HLS-3 (d), HLS-4 (e) and B7T (f)) at different concentrations ( $n=4$ ).

compounds, HLS-3 demonstrated the highest aqueous solubility under all pH conditions.

### 3.2. Cholinesterases inhibition activities of the THA dimers

#### 3.2.1. Inhibition studies on AChE and BChE

The inhibitory activities of the THA dimers were evaluated against AChE and BChE with THA and B7T serving as the two positive controls. Fig. 2 shows the dose-response curves of inhibition on AChE (Fig. 2a) and BChE (Fig. 2b) by the studied compounds. Most of the curves demonstrated a characteristic sigmoidal shape, except for inhibition of BChE by HLS-5 and HLS-6 (due to their relatively low activities). In comparison to THA, all THA dimers produced greater inhibition against AChE and lower inhibition against BChE. These dose-response curves indicated that the studied THA dimers would inhibit AChE more potently and selectively than THA.

To quantitatively describe the inhibition activity of the studied compounds, their  $IC_{50}$  values and selectivity index for inhibition of AChE over BChE were calculated and compared as shown in Fig. 2. Based on the  $IC_{50}$  for the AChE inhibition, THA dimers were up to 300-fold more potent than that of THA. Among the studied THA dimers (HLS-1, HLS-2, HLS-3, HLS-4, HLS-5 and HLS-6), HLS-3 showed the highest activity and selectivity on AChE inhibition, which was similar to that of B7T.

#### 3.2.2. Inhibition type on AChE

Due to the relatively high  $IC_{50}$  values of AChE inhibition, HLS-5 and HLS-6 were not selected for further investigation. In order to identify the type of inhibition, the inhibition of AChE by THA (100, 200 and 400 nM), B7T (0.5, 1 and 2 nM) and four THA dimers (including HLS-1 (3, 6 and 12 nM), HLS-2 (1.5, 3 and 6 nM), HLS-3 (0.5, 1 and 2 nM) and HLS-4 (10, 20 and 40 nM)) were investigated at different concentrations of AChE substrate (0.1, 0.125, 0.2, 0.4 and 0.8 mM). For example, the representative Lineweaver–Burk plots at three different THA concentrations together with control (without inhibitor) were shown in Fig. 3a. The four lines intersecting at the same point in the second quadrant indicated that THA was a mixed type inhibitor, which was consistent with previous observations (Snape et al., 1999; Wang et al., 1999b). The calculated inhibition constant  $K_i$  (the dissociation constant of enzyme–inhibitor complex) and  $K'_i$  (the dissociation constant of enzyme–substrate–inhibitor complex) of THA were determined to

be 355.5 and 473.5 nM, respectively (Fig. 2). Since  $K_i < K'_i$ , the affinity of inhibitor THA towards enzyme (AChE) was higher than that towards the enzyme–substrate complex, which also confirmed that THA was a mixed type inhibitor for AChE. After dimerization, all of the studied THA dimers showed a pattern of mixed inhibition type with much lower inhibition constants than that of THA. Among these dimers, HLS-3 showed the highest inhibition on AChE according to the determined inhibition constants, which was consistent with the finding based on the calculated  $IC_{50}$ .

### 3.3. Investigation of intestinal permeability of THA dimers on Caco-2 monolayer model

#### 3.3.1. Cytotoxicity study of the THA dimers toward Caco-2 cells

The objective of this study was to compare the cytotoxicity of THA dimers toward Caco-2 cells as well as to select the non-toxic concentrations for further transport studies on Caco-2 cell monolayer models. The results shown in Fig. 4 suggested that all tested compounds showed concentration-dependent cytotoxicity. Among the tested compounds, B7T showed the highest cytotoxicity with calculated  $IC_{50}$  value of  $(219.1 \pm 26.8 \mu\text{M})$ , followed by HLS-1  $\approx$  HLS-2  $\approx$  HLS-3  $\approx$  HLS-4  $>$  THA ( $7505 \pm 1269 \mu\text{M}$ ). Since the reproducibility and accuracy of transport studies with *in vitro* cell model relies on the cell functions during the study, it is important that cells remain viable and are not adversely influenced by operation during incubation period (Fix, 1996). Typically, at least 80% cell viability is considered as a minimum to conduct transport study across cell monolayers (Hong et al., 2006; Sandker et al., 1993; Sezgin et al., 2007). According to the cytotoxicity results, two concentrations (30 and 80  $\mu\text{M}$ ) of THA dimers (HLS-1, HLS-2, HLS-3, HLS-4 and B7T) were selected for further transport studies on Caco-2 monolayer models.

#### 3.3.2. Bidirectional transport studies of the THA dimers on Caco-2 monolayer model

The calculated  $P_{app}$  values, cell uptake and efflux ratio (ER) of studied compounds are listed in Table 2. For THA, the absorptive permeability was comparable to that of the transcellular marker propranolol ( $P_{app}$  over  $10^{-5}$  cm/s) with no significant efflux observed (ER of 0.87), indicating that transcellular diffusion was the main pathway for THA to permeate across the Caco-2 cell monolayer. For B7T, its bidirectional transport resulted in a minor efflux with ER of 3.0 and a moderate absorptive  $P_{app}$  ( $2.51 \times 10^{-6}$  cm/s), which was in consistence with our previously report (Zhang et al., 2008). However, relatively high intracellular amount of B7T was found with over 46% and 21% of the related loading dose being trapped in the Caco-2 cell monolayer during its apical to basolateral and basolateral to apical transport, respectively. Such high cell uptake of B7T was probably due to its reported high protein binding of 98.7% towards Caco-2 cell lysate (Zhang et al., 2008).

The absorptive permeabilities of HLS-1, HLS-2, HLS-3 and HLS-4 at two loading concentrations (30 and 80  $\mu\text{M}$ ) were in the range of  $0.11$  to  $0.46 \times 10^{-6}$  cm/s, which were comparable to that of the paracellular marker atenolol ( $0.2 \times 10^{-6}$  cm/s (Artursson, 1990)). In contrast to THA, the secretive permeabilities of HLS-1, HLS-2, HLS-3, HLS-4 and B7T were greatly higher than their corresponding absorptive permeabilities at all studied loading concentrations. Among the studied THA dimers, HLS-1 demonstrated the most intensive efflux transport with ER higher than 20. Medium extent of efflux transport of HLS-2, HLS-3 and B7T were observed with ERs in the range of 3 to 11.4 (Hitchcock, 2012). For all studied THA dimers, their absorptive permeability and ER were in the order of  $B7T > HLS-1 \approx HLS-4 > HLS-3 \approx HLS-2$  and  $HLS-1 > HLS-4 > HLS-2 \approx HLS-3 > B7T$ , respectively.

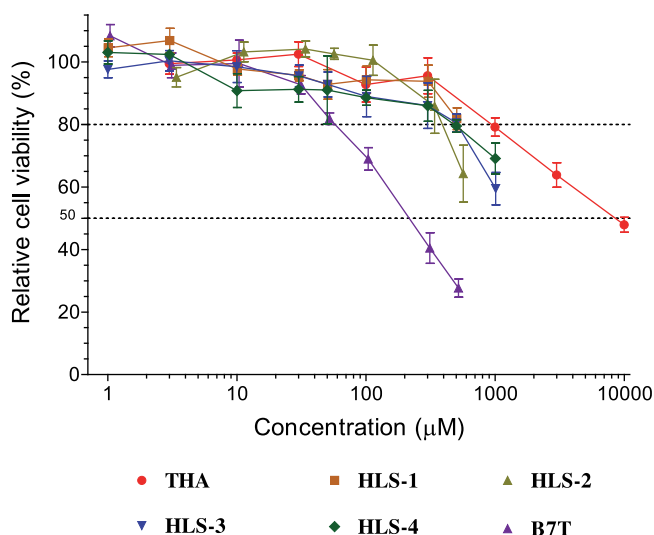


Fig. 4. Cytotoxicities of THA and its dimers toward Caco-2 cells. Each data represents mean  $\pm$  s.d. ( $n = 5$ ).

**Table 2**  
Bidirectional transport and cell uptake of THA dimers in Caco-2 cell model.

Compound	Loading Conc. ( $\mu\text{M}$ )	A–B		B–A		ER <sup>a</sup>
		$P_{\text{app}}$ ( $\times 10^{-6}$ cm/s)	Cell uptake (%)	$P_{\text{app}}$ ( $\times 10^{-6}$ cm/s)	Cell uptake (%)	
HLS-1	30	$0.33 \pm 0.05$	1.26	$12.31 \pm 0.45$	5.96	37.7
	80	$0.46 \pm 0.18$	1.37	$10.81 \pm 0.53$	6.35	23.3
HLS-2	30	N.A.	0.44	$0.63 \pm 0.01$	2.29	N.A.
	80	$0.11 \pm 0.05$	0.76	$0.61 \pm 0.05$	2.23	5.5
HLS-3	30	$0.11 \pm 0.03$	0.62	$0.96 \pm 0.02$	1.04	8.3
	80	$0.15 \pm 0.06$	0.36	$0.68 \pm 0.06$	0.31	4.5
HLS-4	30	$0.37 \pm 0.03$	2.40	$3.14 \pm 0.08$	4.40	8.4
	80	$0.30 \pm 0.06$	1.36	$3.45 \pm 0.51$	5.12	11.4
B7T	30	$2.51 \pm 0.23$	46.9	$7.61 \pm 0.74$	21.1	3.03
	80 <sup>b</sup>	N.D.	N.D.	N.D.	N.D.	N.A.

Note: The determined  $P_{\text{app(A} \rightarrow \text{B)}}$ ,  $P_{\text{app(B} \rightarrow \text{A)}}$ , ER of THA (as control) were  $24.09 \pm 1.14 \times 10^{-6}$  cm/s,  $20.93 \pm 1.02 \times 10^{-6}$  cm/s and 0.87, respectively. N.D.: not determined; N.A.: not applicable.

<sup>a</sup> ER: efflux ratio.

<sup>b</sup> Large number of floating cells were observed and TEER decreased to around  $200 \Omega \text{ cm}^2$  at 60 min after loading B7T at  $80 \mu\text{M}$ , thus, the  $P_{\text{app}}$  and cell uptake at this loading concentration were not determined.

In addition, the bidirectional transport studies demonstrated that all the THA dimers have much lower intestinal permeabilities than that of THA, and could be classified as the low-permeability compounds. The observed medium or high efflux ratio indicated that the limited absorptive permeabilities of THA dimers could be associated with their efflux transport during the absorption processes.

#### 4. Discussion

AChE, the enzyme that hydrolyze the neurotransmitter acetylcholine at cholinergic synapses, is the target of the first generation of drugs approved for the management of AD. AChE has an ellipsoidal shape with 3-D dimensions  $\sim 45 \times 60 \times 65 \text{ \AA}$ , and consists of a 12-stranded central mixed  $\beta$ -sheet surrounded by 14  $\alpha$ -helices (Sussman et al., 1991). X-ray crystallography has identified an active site at the bottom of a narrow gorge. Ser<sup>200</sup>, His<sup>400</sup> and Glu<sup>327</sup> are found to be the three residues at active site forming a planar array, which could resemble the catalytic triad of chymotrypsin and other serine proteases. The active site is believed to be responsible for the choline-binding and catalytic machinery. In addition to catalytic site, a peripheral binding site, located at the opening of the enzyme binding pocket and is far from the catalytic site at the bottom of gorge with distance of  $\sim 20 \text{ \AA}$  long, has also been identified by site-directed mutagenesis (Sussman et al., 1991). Tyr<sup>70</sup>, Trp<sup>279</sup> and Tyr<sup>121</sup> are three conserved aromatic residues found at the peripheral site, increasing the concentration of acetylcholine at the gorge opening and facilitating its delivery to bottom catalytic site. The catalytic site at the bottom and peripheral site at the top of AChE make up the active gorge of this enzyme. Based on the hypothesis of dual binding with catalytic site and peripheral site simultaneously, Pang et al. designed THA dimers with different length of alkene chain linkers by automated computer docking system (Pang et al., 1996). According to the results from their wet lab, the highest AChE inhibition activity was reached by B7T with 7 methylene groups between two THA residues. The heptylene chain allowed the ring nitrogen atoms of the two THA moieties to line up to  $18 \text{ \AA}$  apart, which served a very suitable distance for dual binding of catalytic site and peripheral site of AChE. The high affinity to catalytic site of B7T, together with the binding at peripheral site hindering the entering of the substrate into the lower portion of enzyme gorge, gave a high inhibition activity to AChE (Pang et al., 1996). HLS-1, HLS-2 and HLS-3, consisting similar length of linkers (8 atoms on the line chain between the ring nitrogen atoms of the two THA moieties) with B7T, also demonstrated high AChE inhibition activities ( $\text{IC}_{50}$ : 1.1–7.8 nM, in Fig. 2). HLS-4, with shorter linker (5 atoms on the

line chain), had a lower inhibition activity than that of HLS-3. The impact of the linker length of currently studied THA dimers on inhibition activity was consistent with previously reported THA-toluene hybrids (Pang et al., 1996).

Based on the experimental and computational approaches in estimating solubility and permeability of medication drugs, Lipinski et al. proposed a “Lipinski’s Rule of Five” to evaluate if a chemical compound with certain pharmacological activity has properties that would make it likely an orally active drug in humans (Lipinski et al., 2001). According to the current results of *in silico* prediction of physicochemical properties, the number of hydrogen bond donors and receptors of THA dimers are within the criteria, but the molecular weight and Log *P* values are close to the borderline of “Lipinski’s Rule of Five”. In order to cut down the molecular weight and reduce the Log *P* value, HLS-5 and HLS-6 were designed based on HLS-2 by chopping the hexatomic ring of THA structure. From the predicted values, we found that their Log *P* values decreased and the aqueous solubilities under physiological conditions increased (Table 1). However, after chopping the hexatomic ring of THA structure, the inhibition activities of HLS-5 and HLS-6 on AChE were dramatically decreased by 38-fold and 64-fold in comparison to that of HLS-2, respectively (Fig. 2), which might be explained by the structural change of HLS-5 and HLS-6. From HLS-2 to HLS-5 and HLS-6 (Fig. 1), the 1,2,3,4-tetrahydroacridine regional fragments (Log *P*:  $3.77 \pm 0.2$ ) in HLS-2 were changed to quinoline (Log *P*:  $2.08 \pm 0.2$ ) and 2-methyl-quinoline (Log *P*:  $2.54 \pm 0.2$ ) regional fragments in HLS-5 and HLS-6, respectively (Log *P* calculated by ACD/Lab online program). Such structural changes lead to a decrease of affinity to “esteratic” subsite (Sussman et al., 1991) of AChE catalytic site, hence, decrease in the inhibition activities, which agreed with previous findings (Carlier et al., 1999).

BChE, also known as pseudocholinesterase or nonspecific cholinesterase outside the central nervous system (*i.e.*, in blood), is a serine hydrolase that catalyzes the hydrolysis of esters of choline including butyrylcholine, succinylcholine and acetylcholine (Darvesh et al., 2003). Like AChE, BChE has serine, histidine and glutamic acid residues (Ser<sup>226</sup>, His<sup>466</sup> and Glu<sup>335</sup>, respectively) that are essential for its catalytic activity. Unlike AChE, BChE only contains catalytic site at the bottom of gorge but without peripheral site. Since the peripheral site is absent in BChE, these THA dimers provided a better selectivity toward AChE over BChE in terms of binding property.

By fluorescent probe technique, peripheral site of AChE was believed to act as uncompetitive inhibitor binding site (Li et al., 2009). In addition, the peripheral site provides aromatic guidance by setting an array of low-affinity binding site to ligands (Dvir et al.,

2010). Such low-affinity peripheral binding site of AChE provides a place for the inhibitors binding to enzyme-substrate complex, leading to non-competitive or mixed type of inhibition. Due to different affinity of inhibitors towards free enzyme and enzyme-substrate complex ( $K_i \neq K'_i$ , in Fig. 2), all THA dimers demonstrated a mixed type of inhibition.

To produce beneficial effects in human, drugs should be firstly absorbed and delivered to the pathological site. Except for intravenous administration, other commonly applied administration routes (i.e., oral, intranasal, sublingual, rectal, transdermal, inhalation, etc.) have a physiological barrier consisting of cell layers to form a rate-limiting barrier for the absorption of dissolved drugs. As a consequence, the proper reconstitution of *in vitro* human differentiated epithelial cell monolayers allow the prediction of drug absorption *in vivo*. (i.e., Caco-2 for oral absorption (Hubatsch et al., 2007), Calu-3 for intranasal and inhalation absorption (Foster et al., 2000; Wang et al., 2011) and HO-1-u-1 for sublingual absorption (Wang et al., 2009), etc.) Comparing with THA, all studied THA dimers have relatively low permeabilities across Caco-2 cell monolayers and could be classified as the low permeable compounds. Zhang et al. investigated the intestinal absorption of B7T on Caco-2 cell model and *in situ* rat intestinal perfusion model (Zhang et al., 2008). They found that the absorptive permeability of B7T, with a  $P_{app}$  value of  $\sim 3 \times 10^{-6}$  cm/s, was much lower than that of the transcellular maker propranolol in Caco-2 monolayer model, which was consistent with what we observed in the current study. In the rat *in situ* intestinal perfusion model, B7T was subject to an extensive intestinal extraction (>90%) with extremely low concentration of B7T detected in mesenteric blood, which was further found to be associated with the high tissue binding (99.9%) of B7T (Zhang et al., 2008). Such high tissue binding also resulted in extremely high percentage of B7T trapped within Caco-2 (46.9%) cells in the present study. Such high cellular uptake may lead to the accumulation of B7T in the cells, and hence inhibition/deactivation of the mitochondrial dehydrogenases, resulting in a high cytotoxicity in Caco-2 cells. In contrast to B7T, the cellular uptakes in Caco-2 cells of other studied THA dimers (HLS-1, HLS-2, HLS-3 and HLS-4) were very low (<6.5%) with lower cytotoxicity, which might indicate their potential lower toxicity toward GI tract during oral absorption processes.

In addition, cytotoxicity studies of all synthesized compounds were carried out on HepG2 cell line. It was found that all tested THA dimers were less toxic to HepG2 cells at lower testing concentrations (i.e., 0.1 and 1  $\mu$ M). When the testing concentration was increased to 100  $\mu$ M, HLS-3 and HLS-4 demonstrated significantly lower cytotoxicity than that of B7T (Supplementary file). Although THA showed the lowest cytotoxicity among all the studied compounds, such *in vitro* findings in HepG2 cell line may not be able to represent its *in vivo* situation due to the fact that formation of reactive metabolite (quinone methide) instead of THA itself was proposed to be the mechanism of liver toxicity induced by THA *in vivo* (Park et al., 1994; Patocka et al., 2008). Therefore, the potential *in vivo* liver toxicities of the investigated THA dimers still need further investigations in related animal models.

In summary, during the early stage of discovery for AChE inhibitors, the most ideal drug candidate would have the following characteristics including (1) high anti-AChE activity and selectivity; (2) efficient permeability in Caco-2 monolayer model for good absorption across various membranes; (3) sufficient aqueous solubility for fast dissolution and easy formulation development; (4) low efflux transport for effective drug delivery and (5) minimum cytotoxicity for safe use, etc. (Chen et al., 2006; Kerns and Di, 2008). However, none of the synthesized THA dimers could fulfill all above properties. Therefore, a balanced consideration of

these properties should be taken in selection of the potential candidates for further *in vivo* investigation.

## 5. Conclusion

We have reported the synthesis, anti-cholinesterase inhibition activity, physicochemical properties, cytotoxicity and intestinal permeability of six THA dimers, namely HLS-1, HLS-2, HLS-3, HLS-4, HLS-5 and HLS-6. Based on the  $IC_{50}$  and  $K_i$  values, the *in vitro* AChE inhibition activities of studied THA dimers were up to 300-fold more potent than that of THA. Among the studied THA dimers, HLS-3 showed the highest activity and selectivity on AChE inhibition with a mixed type. It was found that chopping hexatomic ring of THA structure dramatically decreased the AChE inhibition activity. All studied THA dimers showed significantly lower intestinal permeability than that of THA.

## Acknowledgements

Financial support from CUHK 480809 from the Research Grants Council, Hong Kong, China; L. He thanks Hong Kong Ph.D Fellowship, Prof. C.Y. Ho thanks Thousand Young Talents Program for financial support.

## Appendix A. Supplementary data

Supplementary data associated with this article can be found, in the online version, at <http://dx.doi.org/10.1016/j.ijpharm.2014.10.058>.

## References

- Alcala Mdel, M., Vivas, N.M., Hospital, S., Camps, P., Munoz-Torrero, D., Badia, A., 2003. Characterisation of the anticholinesterase activity of two new tacrine-huperzine A hybrids. *Neuropharmacology* 44, 749–755.
- Alonso, D., Dorransoro, I., Rubio, L., Munoz, P., Garcia-Palomo, E., Del Monte, M., Bidon-Chanal, A., Orozco, M., Luque, F.J., Castro, A., Medina, M., Martinez, A., 2005. Donepezil-tacrine hybrid related derivatives as new dual binding site inhibitors of AChE. *Bioorg. Med. Chem.* 13, 6588–6597.
- Artursson, P., 1990. Epithelial transport of drugs in cell culture. I: a model for studying the passive diffusion of drugs over intestinal absorptive (Caco-2) cells. *J. Pharm. Sci.* 79, 476–482.
- Bajda, M., Guzior, N., Ignasik, M., Malawska, B., 2011. Multi-target-directed ligands in Alzheimer's disease treatment. *Curr. Med. Chem.* 18, 4949–4975.
- Balimane, P.V., Han, Y.H., Chong, S., 2006. Current industrial practices of assessing permeability and P-glycoprotein interaction. *AAPS J.* 8, E1–13.
- Bolognesi, M.L., Cavalli, A., Valgimigli, L., Bartolini, M., Rosini, M., Andrisano, V., Recanatini, M., Melchiorre, C., 2007. Multi-target-directed drug design strategy: from a dual binding site acetylcholinesterase inhibitor to a trifunctional compound against Alzheimer's disease. *J. Med. Chem.* 50, 6446–6449.
- Carlier, P.R., Chow, E.S., Han, Y., Liu, J., El Yazal, J., Pang, Y.P., 1999. Heterodimeric tacrine-based acetylcholinesterase inhibitors: investigating ligand-peripheral site interactions. *J. Med. Chem.* 42, 4225–4231.
- Cavalli, A., Bolognesi, M.L., Minarini, A., Rosini, M., Tumiatti, V., Recanatini, M., Melchiorre, C., 2008. Multi-target-directed ligands to combat neurodegenerative diseases. *J. Med. Chem.* 51, 347–372.
- Chao, X., He, X., Yang, Y., Zhou, X., Jin, M., Liu, S., Cheng, Z., Liu, P., Wang, Y., Yu, J., Tan, Y., Huang, Y., Qin, J., Rapposelli, S., Pi, R., 2012. Design: synthesis and pharmacological evaluation of novel tacrine-caffeic acid hybrids as multi-targeted compounds against Alzheimer's disease. *Bioorg. Med. Chem. Lett.* 22, 6498–6502.
- Chen, X.Q., Antman, M.D., Gesenberg, C., Gudmundsson, O.S., 2006. Discovery pharmaceuticals – challenges and opportunities. *AAPS J.* 8, E402–408.
- Darvesh, S., Hopkins, D.A., Geula, C., 2003. Neurobiology of butyrylcholinesterase. *Nat. Rev. Neurosci.* 4, 131–138.
- Dvir, H., Silman, I., Harel, M., Rosenberry, T.L., Sussman, J.L., 2010. Acetylcholinesterase: from 3D structure to function. *Chem.-Biol. Interact.* 187, 10–22.
- Ellman, G.L., Courtney, K.D., Andres Jr., V., Feather-Stone, R.M., 1961. A new and rapid colorimetric determination of acetylcholinesterase activity. *Biochem. Pharmacol.* 7, 88–95.
- Evin, G., Lessene, G., Wilkins, S., 2011. BACE inhibitors as potential drugs for the treatment of Alzheimer's disease: focus on bioactivity. *Recent Pat. CNS Drug Discov.* 6, 91–106.
- Finney, D.J., 1971. *Probit Analysis: A Statistical Treatment of the Sigmoid Response Curve*. Cambridge University Press, Cambridge, UK.

- Fix, J.A., 1996. Intestinal rings and isolated intestinal mucosal cells. In: Borchardt, R. T., Smith, P.L., Wilson, G. (Eds.), *Models for Assessing Drug Absorption and Metabolism*. Springer, New York, USA, pp. 51–66 (Chapter 4).
- Foster, K.A., Avery, M.L., Yazdani, M., Audus, K.L., 2000. Characterization of the Calu-3 cell line as a tool to screen pulmonary drug delivery. *Int. J. Pharm.* 208, 1–11.
- Fu, H., Li, W., Liu, Y., Lao, Y., Liu, W., Chen, C., Yu, H., Lee, N.T., Chang, D.C., Li, P., Pang, Y., Tsim, K.W., Li, M., Han, Y., 2007. Mitochondrial proteomic analysis and characterization of the intracellular mechanisms of bis(7)-tacrine in protecting against glutamate-induced excitotoxicity in primary cultured neurons. *J. Proteome Res.* 6, 2435–2446.
- Fu, H., Li, W., Luo, J., Lee, N.T., Li, M., Tsim, K.W., Pang, Y., Youdim, M.B., Han, Y., 2008. Promising anti-Alzheimer's dimer bis(7)-tacrine reduces beta-amyloid generation by directly inhibiting BACE-1 activity. *Biochem. Biophys. Res. Commun.* 366, 631–636.
- Goedert, M., Spillantini, M.G., 2006. A century of Alzheimer's disease. *Science* 314, 777–781.
- Guo, Y., Shen, H., 2004. pKa, solubility, and lipophilicity: assessing physicochemical properties of lead compounds. In: Yan, Z., Caldwell, G. (Eds.), *Optimization in Drug Discovery*. Humana Press, Totowa, NJ, USA, pp. 1–17 (Chapter 1).
- Heppner, F.L., Gandy, S., McLaurin, J., 2004. Current concepts and future prospects for Alzheimer disease vaccines. *Alzheimer Dis. Assoc. Disord.* 18, 38–43.
- Hitchcock, S.A., 2012. Structural modifications that alter the P-glycoprotein efflux properties of compounds. *J. Med. Chem.* 55, 4877–4895.
- Hong, S., Leroueil, P.R., Janus, E.K., Peters, J.L., Kober, M.M., Islam, M.T., Orr, B.G., Baker Jr., J.R., Banaszak Holl, M.M., 2006. Interaction of polycationic polymers with supported lipid bilayers and cells: nanoscale hole formation and enhanced membrane permeability. *Bioconjug. Chem.* 17, 728–734.
- Hubatsch, I., Ragnarsson, E.G., Artursson, P., 2007. Determination of drug permeability and prediction of drug absorption in Caco-2 monolayers. *Nat. Protoc.* 2, 2111–2119.
- Jeong, J.M., Choi, C.H., 2007. Enhancement of paclitaxel transport and cytotoxicity by 7,3',4'-trimethoxyflavone, a P-glycoprotein inhibitor. *J. Pharm. Pharm. Sci.* 10, 547–553.
- Kerns, E.H., Di, L., 2008. *Drug-Like Properties: Concepts, Structure Design and Methods: From ADME to Toxicity Optimization*. Academic Press, Burlington, MA, USA.
- Li, C.R., Zhang, L., Zhou, L.M., Wo, S.K., Lin, G., Zuo, Z., 2012. Comparison of intestinal absorption and disposition of structurally similar bioactive flavones in *Radix Scutellariae*. *AAPS J.* 14, 23–34.
- Li, W., Lee, N.T., Fu, H., Kan, K.K., Pang, Y., Li, M., Tsim, K.W., Li, X., Han, Y., 2006. Neuroprotection via inhibition of nitric oxide synthase by bis(7)-tacrine. *Neuroreport* 17, 471–474.
- Li, W., Mak, M., Jiang, H., Wang, Q., Pang, Y., Chen, K., Han, Y., 2009. Novel anti-Alzheimer's dimer bis(7)-cognitin: cellular and molecular mechanisms of neuroprotection through multiple targets. *Neurotherapeutics* 6, 187–201.
- Li, W., Pi, R., Chan, H.H., Fu, H., Lee, N.T., Tsang, H.W., Pu, Y., Chang, D.C., Li, C., Luo, J., Xiong, K., Li, Z., Xue, H., Carlier, P.R., Pang, Y., Tsim, K.W., Li, M., Han, Y., 2005. Novel dimeric acetylcholinesterase inhibitor bis(7)-tacrine, but not donepezil, prevents glutamate-induced neuronal apoptosis by blocking N-methyl-D-aspartate receptors. *J. Biol. Chem.* 280, 18179–18188.
- Li, W., Xue, J., Niu, C., Fu, H., Lam, C.S., Luo, J., Chan, H.H., Xue, H., Kan, K.K., Lee, N.T., Li, C., Pang, Y., Li, M., Tsim, K.W., Jiang, H., Chen, K., Li, X., Han, Y., 2007. Synergistic neuroprotection by bis(7)-tacrine via concurrent blockade of N-methyl-D-aspartate receptors and neuronal nitric-oxide synthase. *Mol. Pharmacol.* 71, 1258–1267.
- Lipinski, C.A., Lombardo, F., Dominy, B.W., Feeney, P.J., 2001. Experimental and computational approaches to estimate solubility and permeability in drug discovery and development settings. *Adv. Drug Deliv. Rev.* 46, 3–26.
- Liu, J., Ho, W., Lee, N.T., Carlier, P.R., Pang, Y., Han, Y., 2000. Bis(7)-tacrine a novel acetylcholinesterase inhibitor, reverses AF64A-induced deficits in navigational memory in rats. *Neurosci. Lett.* 282, 165–168.
- Malík, I., Sedlářová, E., Csöllei, J., Andriamainty, F., Čížmárik, J., 2007. Relationship between physicochemical properties lipophilicity parameters, and local anesthetic activity of dibasic esters of phenylcarbamic acid. *Chem. Pap.* 61, 206–213.
- Mehta, M., Adem, A., Sabbagh, M., 2012. New acetylcholinesterase inhibitors for Alzheimer's disease. *Int. J. Alzheimer's Dis.* 728983.
- Minarini, A., Milelli, A., Tumiatti, V., Rosini, M., Simoni, E., Bolognesi, M.L., Andrisano, V., Bartolini, M., Motori, E., Angeloni, C., Hrelia, S., 2012. Cystamine-tacrine dimer: a new multi-target-directed ligand as potential therapeutic agent for Alzheimer's disease treatment. *Neuropharmacology* 62, 997–1003.
- Mosmann, T., 1983. Rapid colorimetric assay for cellular growth and survival: application to proliferation and cytotoxicity assays. *J. Immunol. Methods* 65, 55–63.
- Nakao, K., Fujikawa, M., Shimizu, R., Akamatsu, M., 2009. QSAR application for the prediction of compound permeability with in silico descriptors in practical use. *J. Comput. Aided Mol. Des.* 23, 309–319.
- Ng, S.P., Wong, K.Y., Zhang, L., Zuo, Z., Lin, G., 2005. Evaluation of the first-pass glucuronidation of selected flavones in gut by Caco-2 monolayer model. *J. Pharm. Pharm. Sci.* 8, 1–9.
- Padilla, S., Lassiter, T.L., Hunter, D., 1999. Biochemical measurement of cholinesterase activity. In: Harry, J., Tilson, H. (Eds.), *Neurodegeneration Methods and Protocols*. Humana Press, pp. 237–245.
- Pang, Y.P., Quiram, P., Jelacic, T., Hong, F., Brimijoin, S., 1996. Highly potent, selective, and low cost bis-tetrahydroaminacrine inhibitors of acetylcholinesterase. Steps toward novel drugs for treating Alzheimer's disease. *J. Biol. Chem.* 271, 23646–23649.
- Park, B.K., Madden, S., Spaldin, V., Woolf, T.F., Pool, W.F., 1994. Tacrine transaminitis: potential mechanisms. *Alzheimer Dis. Assoc. Disord.* 8, S39–S49.
- Patocka, J., Jun, D., Kuca, K., 2008. Possible role of hydroxylated metabolites of tacrine in drug toxicity and therapy of Alzheimer's disease. *Curr. Drug Metab.* 9, 332–335.
- Pi, R., Mao, X., Chao, X., Cheng, Z., Liu, M., Duan, X., Ye, M., Chen, X., Mei, Z., Liu, P., Li, W., Han, Y., 2012. Tacrine-6-ferulic acid, a novel multifunctional dimer, inhibits amyloid-beta-mediated Alzheimer's disease-associated pathogenesis in vitro and in vivo. *PLoS One* 7, e31921.
- Reisberg, B., Doody, R., Stoffler, A., Schmitt, F., Ferris, S., Mobius, H.J., Memantine Study Group, 2003. Memantine in moderate-to-severe Alzheimer's disease. *N. Engl. J. Med.* 348, 1333–1341.
- Robinson, D.M., Keating, G.M., 2006. Memantine – a review of its use in Alzheimer's disease. *Drugs* 66, 1515–1534.
- Sandker, G.W., Weert, B., Merema, M.T., Kuipers, W., Slooff, M.J., Meijer, D.K., Groothuis, G.M., 1993. Maintenance of viability and transport function after preservation of isolated rat hepatocytes in various simplified University of Wisconsin solutions. *Biochem. Pharmacol.* 46, 2093–2096.
- Sezgin, Z., Yuksel, N., Baykara, T., 2007. Investigation of pluronic and PEG-PE micelles as carriers of meso-tetraphenyl porphine for oral administration. *Int. J. Pharm.* 332, 161–167.
- Shu, X.J., Liu, W., Zhang, L., Yang, R., Yi, H.L., Li, C.L., Ye, Y.J., Ai, Y.X., 2012. Effect of bis(7)-tacrine on cognition in rats with chronic cerebral ischemia. *Neurosci. Lett.* 512, 103–108.
- Snape, M.F., Misra, A., Murray, T.K., De Souza, R.J., Williams, J.L., Cross, A.J., Green, A. R., 1999. A comparative study in rats of the in vitro and in vivo pharmacology of the acetylcholinesterase inhibitors tacrine, donepezil and NXX-066. *Neuropharmacology* 38, 181–193.
- Standridge, J.B., 2004. Pharmacotherapeutic approaches to the treatment of Alzheimer's disease. *Clin. Ther.* 26, 615–630.
- Sussman, J.L., Harel, M., Frolow, F., Oefner, C., Goldman, A., Toker, L., Silman, I., 1991. Atomic structure of acetylcholinesterase from *torpedo californica*: a prototypic acetylcholine-binding protein. *Science* 253, 872–879.
- Svensson, A.L., Nordberg, A., 1998. Tacrine and donepezil attenuate the neurotoxic effect of A beta(25–35) in rat PC12 cells. *Neuroreport* 9, 1519–1522.
- Tang, X.C., Han, Y.F., 1999. Pharmacological profile of huperzine A: a novel acetylcholinesterase inhibitor from Chinese herb. *CNS Drug Rev.* 5, 281–300.
- Terry Jr., A.V., Buccafusco, J.J., 2003. The cholinergic hypothesis of age and Alzheimer's disease-related cognitive deficits: recent challenges and their implications for novel drug development. *J. Pharmacol. Exp. Ther.* 306, 821–827.
- Tumiatti, V., Minarini, A., Bolognesi, M.L., Milelli, A., Rosini, M., Melchiorre, C., 2010. Tacrine derivatives and Alzheimer's disease. *Curr. Med. Chem.* 17, 1825–1838.
- Voisin, T., Reynish, E., Portet, F., Feldman, H., Vellas, B., 2004. What are the treatment options for patients with severe Alzheimer's disease? *CNS Drugs* 18, 575–583.
- Wang, H., Carlier, P.R., Ho, W.L., Lee, N.T., Pang, Y.P., Han, Y.F., 1999a. Attenuation of scopolamine-induced deficits in navigational memory performance in rats by bis(7)-tacrine, a novel dimeric AChE inhibitor. *Zhongguo Yao Li Xue Bao* 20, 211–217.
- Wang, H., Carlier, P.R., Ho, W.L., Wu, D.C., Lee, N.T., Li, C.P., Pang, Y.P., Han, Y.F., 1999b. Effects of bis(7)-tacrine, a novel anti-Alzheimer's agent, on rat brain AChE. *Neuroreport* 10, 789–793.
- Wang, S., Chow, M.S., Zuo, Z., 2011. An approach for rapid development of nasal delivery of analgesics—identification of relevant features in vitro screening and in vivo verification. *Int. J. Pharm.* 420, 43–50.
- Wang, Y., Zuo, Z., Chow, M.S., 2009. HO-1-u-1 model for screening sublingual drug delivery-influence of pH: osmolarity and permeation enhancer. *Int. J. Pharm.* 370, 68–74.
- Yang, Y.X., Liu, X., Huang, J.J., Zhong, Y.M., Mao, Z., Xiao, H., Li, M., Zhuo, Y.H., 2012. Inhibition of p38 mitogen-activated protein kinase phosphorylation decrease tert-butyl hydroperoxide-induced apoptosis in human trabecular meshwork cells. *Mol. Vis.* 18, 2127–2136.
- Yu, H., Li, W.M., Kan, K.K., Ho, J.M., Carlier, P.R., Pang, Y.P., Gu, Z.M., Zhong, Z., Chan, K., Wang, Y.T., Han, Y.F., 2008. The physicochemical properties and the in vivo AChE inhibition of two potential anti-Alzheimer agents, bis(12)-hupyrindone and bis(7)-tacrine. *J. Pharm. Biomed. Anal.* 46, 75–81.
- Zhang, L., Lin, G., Kovacs, B., Jani, M., Krajcsi, P., Zuo, Z., 2007. Mechanistic study on the intestinal absorption and disposition of baicalein. *Eur. J. Pharm. Sci.* 31, 221–231.
- Zhang, L., Yu, H., Li, W.M., Cheung, M.C., Pang, Y.P., Gu, Z.M., Chan, K., Wang, Y.T., Zuo, Z., Han, Y.F., 2008. Preclinical characterization of intestinal absorption and metabolism of promising anti-Alzheimer's dimer bis(7)-tacrine. *Int. J. Pharm.* 357, 85–94.